Experimental and theoretical investigation of 3-amino-1,2,4-triazole-5-thiol as a corrosion inhibitor for carbon steel in HCl medium

ARTICLE *in* CORROSION SCIENCE · DECEMBER 2011

Impact Factor: 4.42 · DOI: 10.1016/j.corsci.2011.08.038

4 AUTHORS, INCLUDING:

Başak Doğru Mert
Cukurova University
13 PUBLICATIONS **161** CITATIONS
SEE PROFILE

Gülfeza Kardaş
Cukurova University
62 PUBLICATIONS **1,878** CITATIONS
SEE PROFILE

B. Yazici
Cukurova University
78 PUBLICATIONS **1,858** CITATIONS
SEE PROFILE

Corrosion Science 53 (2011) 4265–4272

Contents lists available at SciVerse ScienceDirect

Corrosion Science

journal homepage: www.elsevier.com/locate/corsci

Experimental and theoretical investigation of 3-amino-1,2,4-triazole-5-thiol as a corrosion inhibitor for carbon steel in HCl medium

Başak Doğru Mert *, M. Erman Mert, Gülfeza Kardaş, Birgül Yazıcı

Çukurova University, Science and Letters Faculty, Chemistry Department, 01330 Balcalı, Adana, Turkey

ARTICLE INFO

Article history:
Received 9 June 2011
Accepted 26 August 2011
Available online 31 August 2011

Keywords:
A. Steel
B. EIS
B. Electrochemical calculation
C. Acid corrosion

ABSTRACT

The inhibition effect of 3-amino-1,2,4-triazole-5-thiol (3ATA5T) was investigated in 0.5 M HCl on carbon steel (CS) by electrochemical impedance spectroscopy and potentiodynamic measurements at various concentrations and temperatures. Results showed that the correlation between experimental (inhibition efficiencies, ΔG_{ads}, E_a) and quantum calculation parameters (dipole moment, E_{HOMO}, E_{LUMO}). The high inhibition efficiency was declined in terms of strongly adsorption of protonated inhibitor molecules on the metal surface and forming a protective film.

1. Introduction

Corrosion inhibitors have been widely studied in many industries to reduce the corrosion rate of metal materials in contact with aggressive medium [1–5]. These are generally synthetic organic molecules, which contain nitrogen, sulfur, oxygen and aromatic rings in their structure. The efficiency of these molecules mainly depends on their abilities to be adsorbed on the metal surface with the polar groups acting as the reactive centers [6]. The scientists [7–10] report that the inhibitive properties of organic inhibitors also mainly depend on some physicochemical properties of the molecule, related to its structure and functional groups, to the possible steric effects and electronic density of donor atoms. It is supposed also to depend on the possible interaction of p-orbitals of the inhibitor with d-orbitals of the surface atoms [11]. The various experimental techniques and theoretical methods have been improved to clarify the relation between the efficiency and structural properties of inhibitor molecules [12–15]. The quantum chemical methods and molecular modeling techniques enable the definition of a large number of molecular quantities characterizing the reactivity, shape, and binding properties of a complete molecule as well as of molecular fragments and substituents. The use of theoretical parameters presents two main advantages: firstly, the compounds and their various fragments and substituents can be directly characterized based on their molecular structure only; and secondly, the proposed mechanism of action can be directly accounted for in terms of the chemical reactivity of the compounds under study [16].

Triazole and its derivatives have been widely studied [17–20] in experimental and theoretical researches. They are not only used against corrosion but also preferred for biological activities such as antiviral, antibacterial, antifungal and antituberculous. It is known that most of them were reported as green inhibitor due to environmentally friendly effects [17]. In this study, the kinetic and thermodynamic parameters for carbon steel corrosion and the inhibitive properties of 3-amino-1,2,4-triazole-5-thiol (3ATA5T), were determined. The experimental results were associated with a theoretical method and discussed.

2. Experimental

The electrochemical measurements were carried out using a CHI 604A electrochemical analyzer (serial number 6A721A) under computer control. All the electrochemical studies were carried out in a conventional three-electrode set up, open to the atmosphere. The counter electrode was a platinum sheet (with 2 cm^2 surface area) and Ag/AgCl (3 mol dm^{-3} KCl) electrode was used as the reference. All potentials given in this study were referred to this reference electrode. The working electrodes were carbon steel alloy with following chemical composition (wt.%); 0.17 C, 0.59 Si, 1.60 Mn, 0.04 P and balance with Fe. The surface area of the working electrode was 0.502 cm^2 while the rest of an electrode was isolated with thick polyester block and electrical conductivity was provided by a copper wire. The exposed surface of working electrodes were abraded using emery paper up to 1200 grade prior to each experiment. The experimental tests were performed in 50 mL, 0.5 M HCl solution in the absence and presence of various 3ATA5T concentrations of which molecular structure is given in Fig. 1. The electrochemical experiments were repeated three times.

* Corresponding author. Tel.: +90 322 338 6968; fax: +90 322 338 6070.
E-mail address: bdogru@cu.edu.tr (B.D. Mert).

0010-938X/$ - see front matter © 2011 Elsevier Ltd. All rights reserved.
doi:10.1016/j.corsci.2011.08.038

The concentrations of the inhibitors employed were varied from 0.5 to 10.0 mM. All the test solutions were prepared from analytical-grade chemical reagents in distilled water without further purification. For each experiment, a freshly prepared solution was used. The test solutions were opened to the atmosphere and the temperature was controlled with thermostat (Nuve BS 302 serial number 03-0033). The EIS experiments were conducted in the frequency range with the high limit of 100 kHz and the low limit 0.006 Hz at open circuit potential for various immersion times. The amplitude was 5 mV. The EIS parameters were calculated by fitting the experimental results to an equivalent circuit using ZView software. The linear polarization resistance (LPR) measurements were carried out by recording the electrode potential ±10 mV around open circuit potential with 1 mV s^{-1} scan rate. The polarization resistance (R_p) was determined from the slope of the current–potential curves obtained. Furthermore, the polarization curves were obtained potentiodynamically in the potential range from −0.9 to 0 V(Ag/AgCl) with 1 mV s^{-1} scan rate, under stirred conditions. Theoretical calculations were carried out using density functional theory (DFT) with 6-311++G (d,p) basis set for all atoms with the Gaussian 03W program. Some electronic properties such as energy of the highest occupied molecular orbital (E_{HOMO}), energy of the lowest unoccupied molecular orbital (E_{LUMO}), energy gap (ΔE) between LUMO and HOMO and Mulliken charges on the backbone atoms for 3ATA5T were determined. The optimized molecular structures and HOMO, LUMO surfaces were visualized using Gauss View.

3. Results and discussion

3.1. Electrochemical measurements

Electrochemical impedance spectroscopy is a convenient technique in studying corrosion mechanisms and adsorption phenomena [21]. Generally, the single semi-circular shape is observed in EIS diagrams for the different electrodes in acidic medium [22–29]. As expected from literature, in this study the EIS results were correlated this phenomena.

In Fig. 2, the obviously depressed semi-circular shape with a diameter of 19.68 Ω cm^{-2}, was observed in the Nyquist plot of CS in the absence of 3ATA5T and slightly depressed semi-circular shape with a diameter of 895.57 Ω cm^{-2} was observed in the Nyquist plot of CS in the presence of 10.0 mM 3ATA5T after 1 h immersion time. In the evaluation of EIS measurements, the diameter of Nyquist plot shows the difference in real impedance at lower and higher frequencies and it is considered as a polarization resistance (R_p). As seen from Fig. 2, the impedance response of CS has significantly changed by the addition of 3ATA5T to the corrosive solution and R_p values increased with increasing 3ATA5T concentration.

In order to determine inhibition activity of 3ATA5T, long term EIS analysis were done during 168 h immersion time, and the EIS diagrams of all samples were given in Fig. 3.

In Fig. 3, the R_p value of CS was decreased with increasing immersion period in the absence of 3ATA5T. Another hand in the presence of 3ATA5T, the R_p values were significantly higher. In both figure (Figs. 2 and 3), the deviation from an ideal semicircle

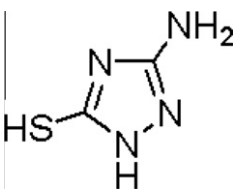

Fig. 1. Chemical structure of 3-amino-1,2,4-triazole-5-thiol (3ATA5T).

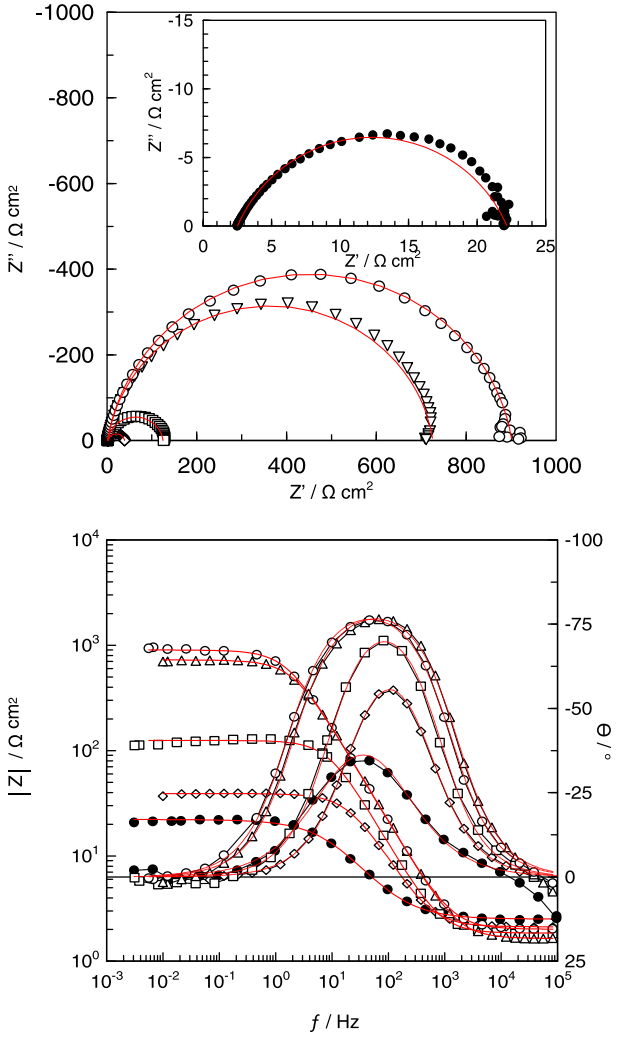

Fig. 2. EIS results of carbon steel electrode obtained in 0.5 M HCl solution (•) (inset) and containing 0.5 (◇), 1.0 (□), 5.0 (△) and 10.0 (○) mM 3ATA5T, after 1 h immersion time. Solid lines show fitted lines.

was generally attributed to the frequency dispersion as well as to the in-homogeneity of the surface and mass transport resistant [30,31]. In Nyquist diagrams, data were dispersed at the low frequency region (Figs. 2 and 3) due to accumulation of inhibitor molecules and/or corrosion products on the CS surface [32–34]. For further information about EIS results, they were clarified and modeled by using ZWiev2 fitting program. The equivalent circuit was shown in Fig. 4 and the calculated values were given in Tables 1 and 2.

In this model (Fig. 4), the R_s is solution resistance, R_p is polarization resistance, which contains charge transfer resistance (R_{ct}), diffuse layer resistance (R_{dl}), inhibitor film resistance (R_f) and all other accumulated kinds (R_a), ($R_p = R_{ct} + R_{dl} + R_f + R_a$). The constant phase element (CPE) was used for fitting, in place of a double layer capacitance (C_{dl}), in order to give a more accurate fit to the experimental results. Generally, the use of a CPE is required due to the distribution of the relaxation times as a result of in-homogeneities present at a micro- or nano-level, such as the surface roughness/porosity, adsorption, or diffusion [35–38].

In Tables, the inhibition efficiency is symbolized as η and calculated with using following equation:

$$\eta\% = \left(\frac{R'_p - R_p}{R'_p}\right) \times 100 \quad (1)$$

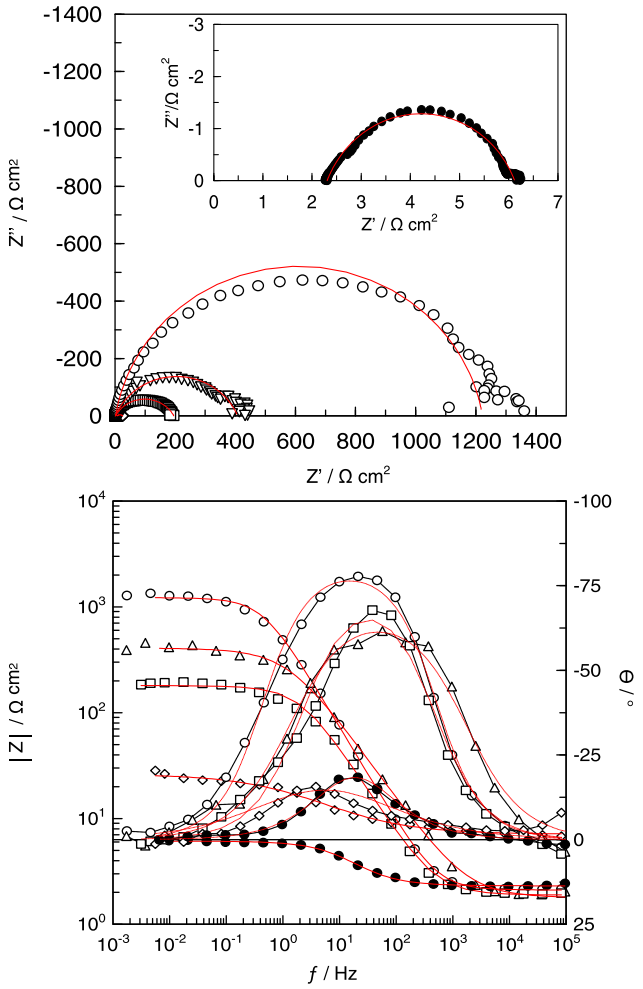

Fig. 3. EIS results of carbon steel electrode obtained in 0.5 M HCl solution (●) (inset) and containing 0.5 (◇), 1.0 (□), 5.0 (△) and 10.0 (○) mM 3ATA5T, after 168 h immersion time. Solid lines show fitted lines.

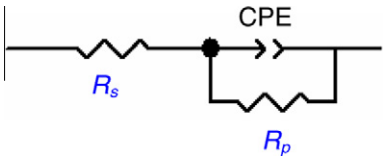

Fig. 4. Electrical equivalent circuit diagrams used to modeling metal/solution interface.

Table 1
Electrochemical parameters for CS corresponding to the EIS and LPR data obtained in 0.5 M HCl solution in the absence and presence of various concentrations of 3ATA5T after 1 h immersion time.

C_{inh}/mM	EIS				LPR	
	R_s/Ω	R_p/Ω cm^2	CPE/μF cm^{-2}	η%	R_p/Ω cm^2	η%
Blank	4.9	19.68	2721		20.58	
0.5	4.2	37.05	3462	46.9	36.14	43.1
1.0	3.7	124.09	1984	84.1	124.98	83.5
5.0	3.3	723.88	1337	97.3	722.88	97.2
10.0	4.1	895.57	1169	97.8	898.08	97.7

where R_p and R'_p are uninhibited and inhibited polarization resistances, respectively. It is clearly seen from Table 1, the η values increase and CPE values decrease with increasing 3ATA5T concentration. In Table 1, the increase in η value is attributed to the formation of protective film on the metal/solution interface [6,39]. According to the Helmholtz model [11], the decrease in CPE can be attributed to the decrease in local dielectric constant and/or increase in the thickness of the electrical double layer (Table 1). The change of these values can be related to the gradual replacement of water molecules by 3ATA5T molecules on the surface and consequently, leads to decrease in the number of active sites necessary for the corrosion reaction [40].

The inhibition efficiency of 3ATA5T has also been evaluated with the help of the linear polarization resistance (LPR) measurements. The R_p values were calculated from the slope of the current–potential curves and given in Table 1. As can be seen from Table 1, the R_p and η values obtained from the LPR measurements are parallel with the EIS measurements.

Particularly during long term immersion, R_p and η values were increased in the presence of inhibitor molecules. In Table 2, the η values were almost constant at 99 during immersion. It suggests the enhancement of adsorption of inhibitor molecules on the CS surface and blocking the surface efficiently [41].

Fig 5 shows the polarization curves of CS in 0.5 M HCl in the absence and presence different concentrations of 3ATA5T. It can be observed that the current density values of CS in the presence of 3ATA5T were lower than in the absence condition. It is clearly seen that the corrosion potential (E_{corr}) values were shifted to nobler values in the presence of 3ATA5T. The observed E_{corr} values were; −0.403, −0.342, −0.349, −0.308, −0.295 mV for 0, 0.5, 1, 5, 10 mM 3ATA5T containing media, respectively. If the displacement in E_{corr} (ΔE_{corr}) vs. Ag/AgCl in the presence of inhibitor, is bigger than 85 mV from E_{corr} vs. Ag/AgCl in the absence medium, the inhibitor can be seen as a cathodic or anodic type; and if displacement is less than 85 mV, the inhibitor can be seen as mixed type. In our study the maximum displacement in (ΔE_{corr} vs. Ag/AgCl value was higher than 85 mV towards anodic region, which indicates the 3ATA5T is anodic inhibitor [42–45]. We note that, the 3ATA5T reduce the anodic dissolution and also retard the hydrogen evolution reaction via blocking the active reaction sites on the metal surface or even can screen the covered part of the electrode and therefore, protect it from the action of the corrosive medium.

Furthermore i_{corr} values were calculated after 168 h immersion by using Stern Geary equation;

$$i_{corr} = B/R_p \quad (2)$$

where R_p is the polarization resistance which were determined from EIS measurements, B is 0.026 V [22,46–48]. The determined values were 6.82×10^{-3}, 1.36×10^{-3}, 0.13×10^{-3}, 6.40×10^{-5}, 2.09×10^{-5} A cm^{-2} for 0, 0.5, 1, 5, 10 mM 3ATA5T containing media, respectively. As it can be italic clearly seen, the calculated i_{corr} values were decreased with increasing 3ATA5T concentration. The inhibition process of 3ATA5T was proposed as a result of a blocking mechanism of the actives sites on the carbon steel surface, which may happen by chemical and/or physical adsorption. It was necessary then to define what processes are likely to occur on the steel surface so that adsorption isotherms were calculated and given in Fig. 6.

The Langmuir adsorption isotherm model has been used extensively in the literature for various metals and inhibitors [49–55]. The plot of C_{inh}/Θ vs. C_{inh} yields a straight line, supporting the assumption that the adsorption of 3ATA5T from HCl solution on the CS surface at the studied temperatures obeys a Langmuir adsorption isotherm, which is represented by the following equation [49–55]:

$$\frac{C_{inh}}{\theta} = \frac{1}{K_{ads}} + C_{inh} \quad (3)$$

Table 2
Electrochemical parameters for CS corresponding to the EIS and LPR data obtained in 0.5 M HCl solution in the absence and presence of 3ATA5T for various immersion times.

Inhibitor	t/h	EIS				LPR	
		R_s/Ω	$R_p/\Omega\ cm^2$	CPE/μF cm^{-2}	η%	$R_p/\Omega\ cm^2$	η%
Blank	24	4.6	9.84	9641		10.54	
	72	4.6	3.87	11,918		3.51	
	120	4.6	3.77	12,008		3.61	
	168	4.6	3.71	11,635		3.51	
3ATA5T	24	3.7	1378.50	189	99.3	1377.49	99.2
	72	3.2	1538.63	237	99.7	1536.62	99.8
	120	4.5	1475.88	265	99.7	1474.37	99.8
	168	4.2	1241.95	319	99.7	1242.45	99.7

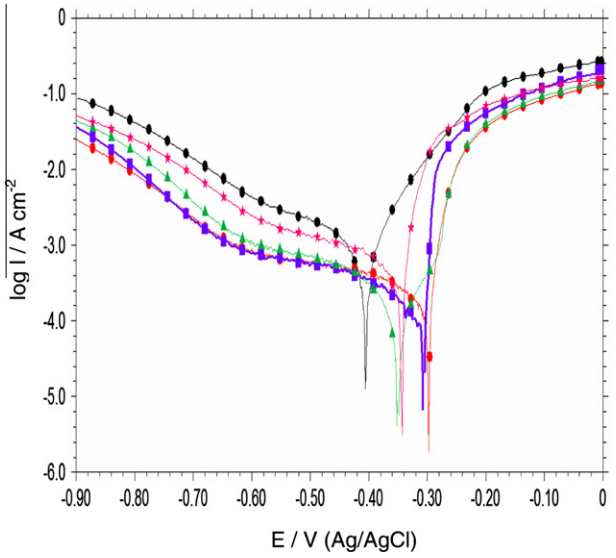

Fig. 5. Polarization plots of CS electrode obtained in 0.5 M HCl solution (●) and containing 0.5 (★), 1.0 (▲), 5.0 (■) and 10.0 (●) mM 3ATA5T after 168 h immersion time.

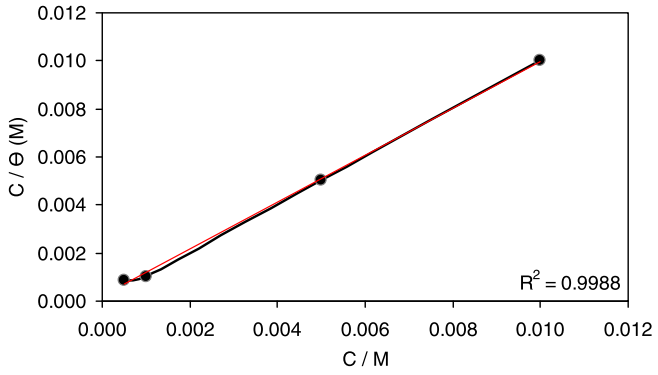

Fig. 6. Langmuir adsorption plot for the CS electrode in 0.5 M HCl containing different concentrations of 3ATA5T.

where C_{inh} is the concentration of inhibitor, Θ is the degree of surface coverage values for various concentrations of the inhibitors in acidic solution; it has been evaluated from the polarization measurements [49]. The K_{ads} is the adsorption equilibrium constant, which is $5 \times 10^3\ M^{-1}$, reflects the high adsorption ability of 3ATA5T on the CS surface. Further, it is related with the standard free energy of adsorption ΔG^O_{ads} according to the following equation:

$$\Delta G^o_{ads} = -RT\ \ln(55.5K_{ads}) \quad (4)$$

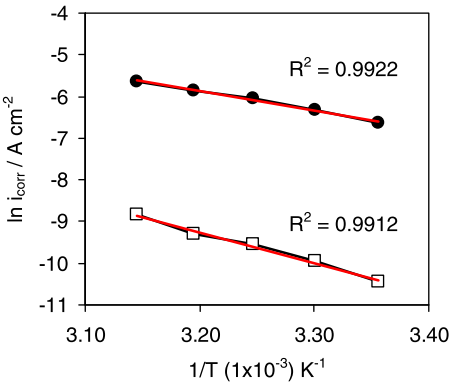

Fig. 7. Arrhenius plots for the CS electrode in the absence (●) and presence (□) of 3ATA5T solutions.

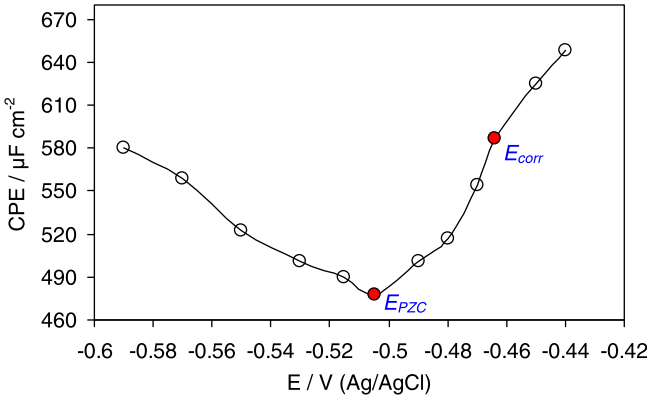

Fig. 8. The plot of CPE vs. applied potential in 10.0 mM 3ATA5T containing 0.5 M HCl solution.

where R is the universal gas constant and T is the absolute temperature, the calculated Δ^o_{ads} is $-31.05\ kJ\ mol^{-1}$. The values of ΔG^O_{ads} around 20 kJ mol^{-1} or lower are consistent with the electrostatic interaction between charged organic molecules and the charged metal surface (physisorption); those around 40 kJ mol^{-1} or higher involve charge sharing or transfer from the organic molecules to the metal surface to form a coordinate type of bond (chemisorption) [56]. The value of ΔG^O_{ads} for 3ATA5T being less than 40 kJ mol^{-1} indicates physical adsorption, in addition to electrostatic interaction, there may be some other interactions [57].

In order to calculate the activation energy of the corrosion process potentiodynamic polarization measurements were performed in the absence and presence of 3ATA5T. The activation energy (E_a) values were calculated by the means of Arrhenius equation;

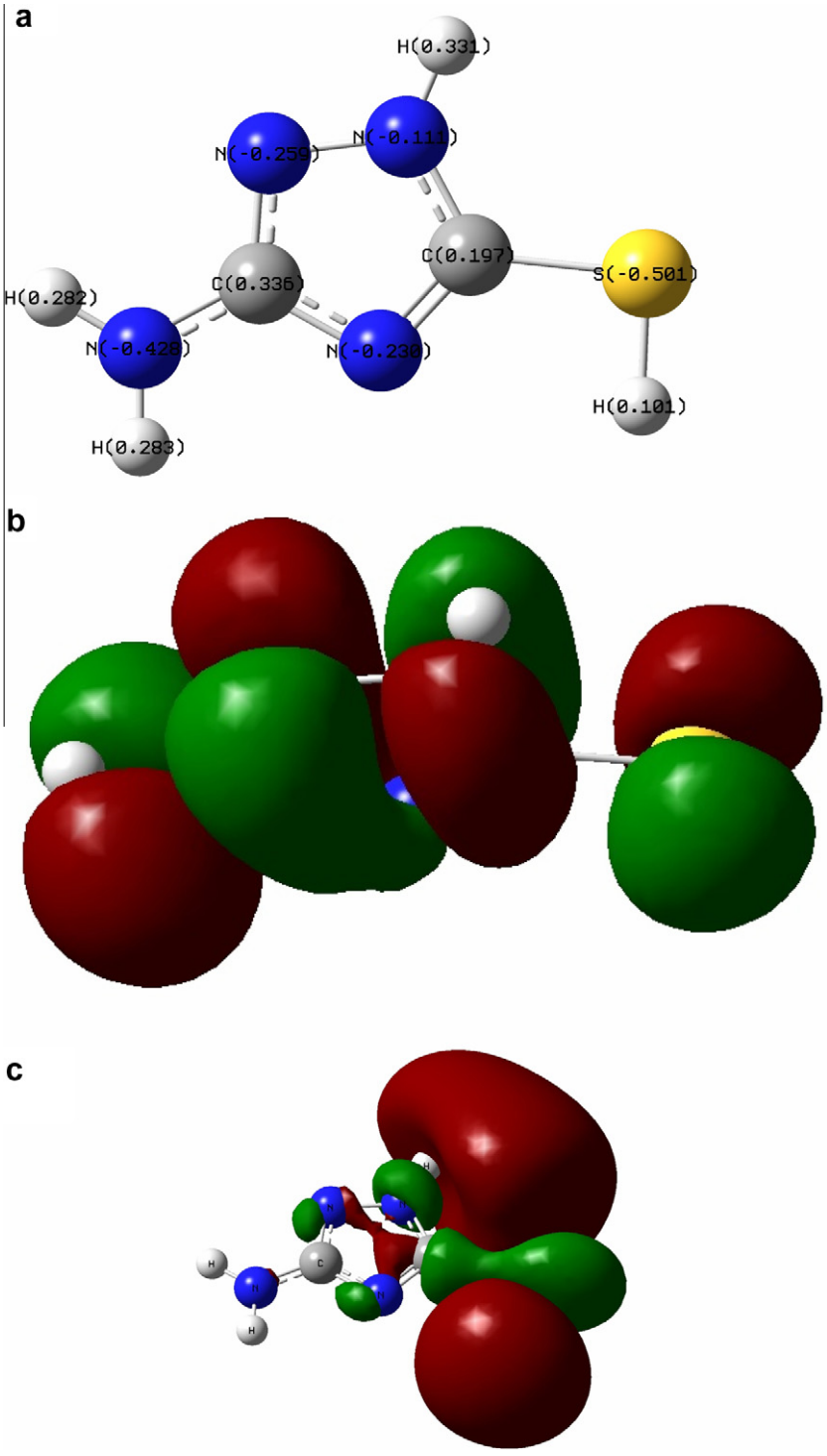

Fig. 9. Optimized molecular structures of neutral 3ATA5T molecule with atomic Mulliken charge values (a), HOMO (b), LUMO (c) orbitals.

$$i_{corr} = A \exp\left(\frac{-E_a}{R.T}\right) \quad (5)$$

where i_{corr} is corrosion current, A is a constant, T is the temperature. The E_a values were determined from the Arrhenius plots (Fig. 7).

The calculated E_a values were 38.30 and 61.20 kJ mol^{-1} for the corrosion process in the absence and presence of 3ATA5T, respectively. The increase in E_a after the addition of the 3ATA5T to the 0.5 M HCl solution indicates that physical adsorption (electrostatic) occurs in the first stage [56,58]. The higher E_a value in the inhibited solution can be correlated with the increased thickness of the double layer, which enhances the activation energy of the corrosion process [56,58].

3.2. Atomic absorption spectroscopy

In order to explain the inhibition behavior of 3ATA5T, not only electrochemical measurements were done, but also the corrosive tests media were analyzed with the atomic absorption spectroscopy (AAS) technique for determination of dissolved iron

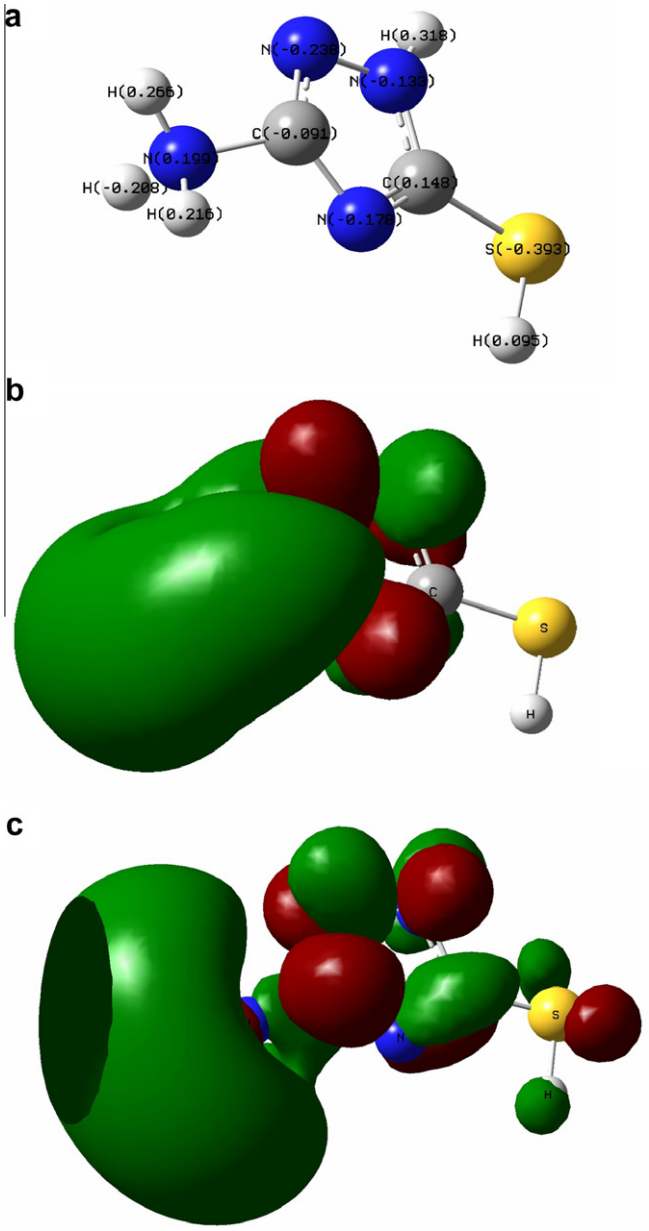

Fig. 10. Optimized molecular structures of second protonated structure (N1-p 3ATA5T) with atomic mulliken charge values (a), HOMO (b), LUMO (c) orbitals.

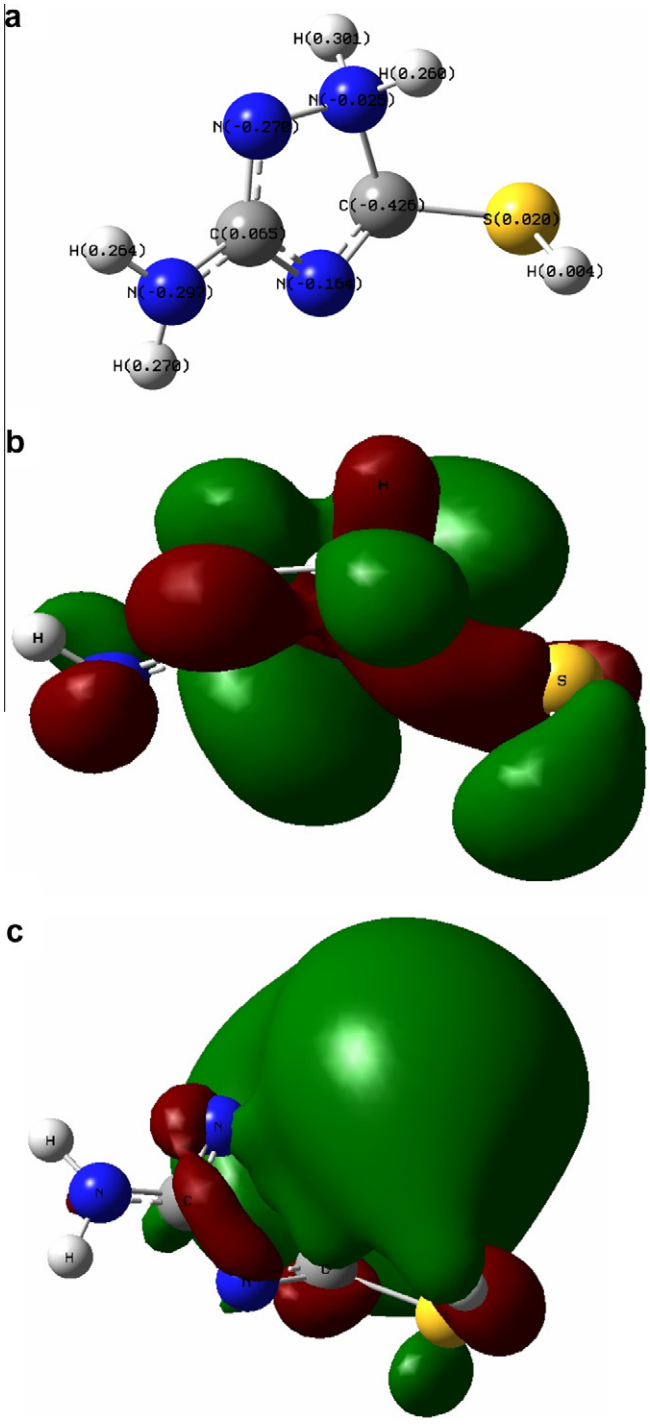

Fig. 11. Optimized molecular structures of second protonated sturucture (N2-p 3ATA5T) with atomic mulliken charge values (a), HOMO (b), LUMO (c) orbitals.

concentrations. For this purpose, all CS electrodes were immersed in the various concentration of 3ATA5T (0, 0.5, 1.0, 5.0, 10.0 mM) containing 0.5 M HCl. All solutions have the same volume (50 mL) and all electrodes were immersed under the same conditions during the 168 h period. After this period electrodes were removed and then all solutions were mixed with diluted HCl in order to solve all the iron compounds in solutions. The percentage Fe ratios were determined as follows: 30898, 10021, 3354, 2259, 155 ppm for 0, 0.5, 1.0, 5.0, 10.0 mM 3ATA5T containing 0.5 HCl solutions, respectively. The AAS results showed that, in the absence of inhibitor molecules, corrosive medium deeply affects and corrodes the CS electrode significantly. On the other hand, in the presence of 3ATA5T dissolved iron concentration decrease obviously. Especially 10.0 mM 3ATA5T containing medium, the dissolved iron values almost 200 times lower than HCl medium. As seen from the AAS results, 3ATA5T effectively inhibits the corrosion of CS in this medium.

Table 3
The calculated quantum chemical parameters for molecular and protonated structures of 3ATA5T.

Molecule	E_{HOMO}/eV	E_{LUMO}/eV	ΔE/eV	μ/Debye
3ATA5T	−5.948	−0.6721	5.2759	0.4301
N1-p 3ATA5T	−2.9113	−0.9693	1.942	0.6351
N2-p 3ATA5T	−4.4344	−0.7742	3.6602	2.3420

The other important phenomenon is clarifying the inhibition mechanism. Organic inhibitors act generally by adsorption on the

metal surface, and their adsorption depend mainly on the surface charge of metal, molecular structure, the charge of inhibitor, solution's chemical composition, nature of metal surface, the temperature, etc. [30,31]. The surface charge of metal can be defined by the position of corrosion potential in respect to the respective potential of zero charge (pzc), which plays a very important role in the electrostatic adsorption process. The EIS offers a good method in order to determine the pzc of metals. For this purpose, EIS study was applied at different potentials and a plot of CPE vs. applied potential was obtained. The plot corresponding to 1 h of exposure time (Fig. 8) shows a minimum value at −0.505 V(Ag/AgCl) which can be called the pzc of CS in 10.0 mM 3ATA5T containing 0.5 M HCl solution.

The corrosion potential of CS in the same conditions is −0.464 V(Ag/AgCl), which is more positive than pzc and indicate positively charged CS surface.

3.3. Theoretical calculations

The quantum chemical calculations were employed to give further insight into the mechanism of inhibition action of 3ATA5T. For this purpose, the highest occupied molecular orbital (E_{HOMO}), energy of the lowest unoccupied molecular orbital (E_{LUMO}), energy gap (ΔE) between LUMO and HOMO and Mulliken charges on the backbone atoms were determined by optimization. The important point is: in the aqueous HCl solution, the 3ATA5T exist either as neutral or/and as a protonated molecules. In pzc measurements, it was determined that the surface of CS was positively charged in 3ATA5T containing HCl solution. In order to give detailed information, all theoretical calculations were obtained for both structures and the optimized molecular (3ATA5T) and protonated structures (for all options: N1-p 3ATA5T and N2-p 3ATA5T) were given in Figs. 9–11.

The calculated parameters such as E_{HOMO}, E_{LUMO} and the dipole moment (μ) of the three structures were shown in Table 3. E_{HOMO} often indicates the electron donating ability of the molecule and the inhibition efficiency increases with increasing E_{HOMO} values. High E_{HOMO} values indicate that the molecule has a tendency to donate electrons to appropriate acceptor molecules with low energy empty molecular orbitals. Increasing of the values of the E_{HOMO} facilitates adsorption (and therefore inhibition) by influencing on the transport process through the adsorbed layer. The energy gap between LUMO and HOMO (ΔE) is a parameter with the smaller value causes higher inhibition efficiencies of the molecule [5,13]. Table 3 shows a higher dipole moment for protonated 3ATA5T molecules in comparison to neutral 3ATA5T. The increase of the dipole moment can lead to increase of inhibition, which could be related to the dipole–dipole interaction of molecules and metal surface [5]. As shown from Table 3, the theoretical calculations supported the pzc measurements. This further provide evidence that the sulfur atom in 3ATA5T was the main center of adsorption with the carbon steel surface, Mulliken charge analysis was carried out (Figs. 9–11). It is clear that the sulfur atom of 3ATA5T has considerable excess of negative charge than other atoms. Thus, the adsorption of 3ATA5T on the metal surface can occur directly involving the displacement of molecules with water from the metal surface [5].

$$Org_{(sol)} + xH_2O \rightarrow Org_{(ads)} + xH_2O_{(sol)} \quad (6)$$

where $Org_{(sol)}$ and $Org_{(ads)}$ are organic molecules in the solution and adsorbed on the metal surface, respectively. x is the number of water molecules replaced by the organic molecules. [23,56]. It should be noted that 3ATA5T adsorb mainly through electrostatic interactions between the negatively charged sulfur atom and the positively charged metal surface (physisorption). The protonated structure (Fig. 10) was probably occurred in the acidic medium so the protonated N-terminal of the molecule may attract the other inhibitor molecules with interaction between the negative S-terminal, in this way the accumulation may occur on the surface.

4. Conclusions

Assessing results of electrochemical techniques as well as surface analysis and quantum chemistry led to the following conclusions:

1. EIS measurements depicted increase of polarization resistance (R_p) and constant phase element (CPE) decline in the presence of 3-amino-1,2,4-triazole-5-thiol (3ATA5T) confirming adsorption of these molecules on the surface.
2. Evaluation of polarization measurements revealed that 3ATA5T suppress cathodic and anodic polarization reactions.
3. The inhibition efficiency values, which were determined both EIS and LPR data, are higher than 99% after 168 h at 10.0 mM inhibitor containing 0.5 M HCl.
4. The adsorption of inhibitor molecules on the carbon steel (CS) surface obeys a Langmuir adsorption isotherm.
5. The value of adsorption equilibrium constant suggested that 3ATA5T is strongly adsorbed on the CS surface. The values of E_a and ΔG_{ads} indicated that the adsorption is seen more a physical form than chemical adsorption.
6. The potential zero charge (pzc) results showed that the CS surface was positively charged in the presence of 3ATA5T. Furthermore, quantum chemical calculations supported the pzc measurements.
7. The calculated quantum parameters reveal that protonated structure (N1-p 3ATA5T) was probably occurred in the acidic medium and inhibited the corrosion reaction significantly.

Consequently, all results show that 3ATA5T is a convenient inhibitor molecule against corrosion of carbon steel in HCl medium.

Acknowledgements

This study has been financially supported by the Cukurova University research fund. The authors are greatly thankful to Çukurova University Research fund. The authors also thank to The Scientific and Technical Research Council of Turkey (TUBITAK).

References

[1] A.S. Machin, J.Y. Mann, Water displacing organic corrosion inhibitors their effect on the fatigue characteristics of aluminium alloy bolted joints, Int. J. Fatigue 4 (1982) 199–208.
[2] M. Christov, A. Popova, Adsorption characteristics of corrosion inhibitors from corrosion rate measurements, Corros. Sci. 46 (2004) 1613–1620.
[3] A. Nagiub, F. Mansfeld, Evaluation of corrosion inhibition of brass in chloride media using EIS and ENA, Corros. Sci. 43 (2001) 2147–2171.
[4] P.C. Okafor, X. Liu, Y.G. Zheng, Corrosion inhibition of mild steel by ethylamino imidazoline derivative in CO_2-saturated solution, Corros. Sci. 51 (2009) 761–768.
[5] L. Herrag, B. Hammouti, S. Elkadiri, A. Aouniti, C. Jama, H. Vezin, F. Bentiss, Adsorption properties and inhibition of mild steel corrosion in hydrochloric solution by some newly synthesized diamine derivatives: experimental and theoretical investigations, Corros. Sci. 52 (2010) 3042–3051.
[6] L. Elkadi, B. Mernari, M. Traisnel, F. Bentiss, M. Lagrenee, The inhibition action of 3,6-bis(2-methoxyphenyl)-1,2-dihydro-1,2,4,5-tetrazine on the corrosion of mild steel in acidic media, Corros. Sci. 42 (2000) 703–719.
[7] E.M. Sherif, A.M. El Shamy, M.M. Ramla, A.O.H. El Nazhawy, 5-(Phenyl)-4H-1,2,4-triazole-3-thiol as a corrosion inhibitor for copper in 3.5% NaCl solutions, Mater. Chem. Phys. 102 (2007) 231–239.
[8] E.M. Sherif, S.M. Park, Effects of 2-amino-5-ethylthio-1,3,4-thiadiazole on copper corrosion as a corrosion inhibitor in aerated acidic pickling solutions, Electrochim. Acta 51 (2006) 6556–6562.

[9] Y. Abboud, A. Abourriche, T. Saffaj, M. Berrada, M. Charrouf, A. Bennamara, A. Cherqaoui, D. Takky, The inhibition of mild steel corrosion in acidic medium by 2,20-bis(benzimidazole), Appl. Surf. Sci. 252 (2006) 8178–8184.

[10] S. Zhang, Z. Tao, S. Liao, F. Wu, Substitutional adsorption isotherms and corrosion inhibitive properties of some oxadiazol-triazole derivative in acidic solution, Corros. Sci. 52 (2010) 3126–3132.

[11] Y. Tang, X. Yang, W. Yang, R. Wan, Y. Chen, X. Yin, A preliminary investigation of corrosion inhibition of mild steel in 0.5 M H_2SO_4 by 2-amino-5-(n-pyridyl)-1,3,4-thiadiazole polarization, EIS and molecular dynamics simulations, Corros. Sci. 52 (2010) 1801–1808.

[12] H. Ju, Z.P. Kai, Y. Li, Aminic nitrogen-bearing polydentate Schiff base compounds as corrosion inhibitors for iron in acidic media: a quantum chemical calculation, Corros. Sci. 50 (2008) 865–871.

[13] I.B. Obot, N.O. Obi-Egbedi, Adsorption properties and inhibition of mild steel corrosion in sulphuric acid solution by ketoconazole: experimental and theoretical investigation, Corros. Sci. 52 (2010) 198–204.

[14] N. Khalil, Quantum chemical approach of corrosion inhibition, Electrochim. Acta 48 (2003) 2635–2640.

[15] E. Jamalizadeh, S.M.A. Hosseini, A.H. Jafari, Quantum chemical studies on corrosion inhibition of some lactones on mild steel in acid media, Corros. Sci. 51 (2009) 1428–1435.

[16] G. Gece, The use of quantum chemical methods in corrosion inhibitor studies, Corros. Sci. 50 (2008) 2981–2992.

[17] H.L. Wang, R.B. Liu, J. Xin, Inhibiting effects of some mercapto-triazole derivatives on the corrosion of mild steel in 1.0 M HCl medium, Corros. Sci. 46 (2004) 2455–2466.

[18] L. Wang, Inhibition of mild steel corrosion in phosphoric acid solution by triazole derivatives, Corros. Sci. 48 (2006) 608–616.

[19] A.Y. Musa, A.A.H. Kadhum, A.B. Mohamad, M.S. Takriff, A.R. Daud, S.K. Kamarudin, On the inhibition of mild steel corrosion by 4-amino-5-phenyl-4H-1,2,4-trizole-3-thiol, Corros. Sci. 52 (2010) 526–533.

[20] M.L. Zheludkevich, K.A. Yasakau, S.K. Poznyak, M.G.S. Ferreira, Triazole and thiazole derivatives as corrosion inhibitors for AA2024 aluminium alloy, Corros. Sci. 47 (2005) 3368–3383.

[21] R. Touir, N. Dkhireche, M. Ebn Touhami, M. Lakhrissi, B. Lakhrissi, M. Sfaira, Corrosion and scale processes and their inhibition in simulated cooling water systems by monosaccharides derivatives Part I: EIS study, Desalination 249 (2009) 922–928.

[22] R.G. Kelly, J.R. Scully, D.W. Shoesmith, R.G. Buchheit, Electrochemical Techniques in Corrosion Science and Engineering, Marcel Dekker, Inc., New York, 2003. 127, 290–302.

[23] J. Bockris, A.K.N. Reddy, M. Gamboa-Aldeco, Modern Electrochemistry Fundamentals of Electrodics, second ed., Kluwer Academic/Plenum Publishers, New York, 2000. pp. 871–890, 973–975.

[24] A. Ostovari, S.M. Hoseinieh, M. Peikari, S.R. Shadizadeh, S.J. Hashemi, Corrosion inhibition of mild steel in 1 M HCl solution by henna extract: a comparative study of the inhibition by henna and its constituents (Lawsone, gallic acid, a-D-glucose and tannic acid), Corros. Sci. 51 (2009) 1935–1949.

[25] M.S. Morad, A.A.O. Sarhan, Application of some ferrocene derivatives in the field of corrosion inhibition, Corros. Sci. 50 (2008) 744–753.

[26] S. John, B. Joseph, K.K. Aravindakshan, A. Joseph, Inhibition of mild steel corrosion in 1 M hydrochloric acid by 4-(*N*,*N*-dimethylaminobenzilidine)-3-mercapto-6-methyl-1,2,4-triazin(4H)-5-one (DAMMT), Mater. Chem. Phys. 122 (2010) 374–379.

[27] K.S. Jacob, G. Parameswaran, Corrosion inhibition of mild steel in hydrochloric acid solution by Schiff base furoin thiosemicarbazone, Corros. Sci. 52 (2010) 224–228.

[28] I. Ahamad, M.A. Quraishi, Bis (benzimidazol-2-yl) disulphide: an efficient water soluble inhibitor for corrosion of mild steel in acid media, Corros. Sci. 51 (2009) 2006–2013.

[29] S. Zhang, Z. Tao, W. Li, B. Hou, The effect of some triazole derivatives as inhibitors for the corrosion of mild steel in 1 M hydrochloric acid, Appl. Surf. Sci. 255 (2009) 6757–6763.

[30] W. Li, Q. He, C. Pei, B. Hou, Experimental and theoretical investigation of the adsorption behaviour of new triazole derivatives as inhibitors for mild steel corrosion in acid media, Electrochim. Acta 52 (2007) 6386–6394.

[31] B.D. Mert, B. Yazıcı, The electrochemical synthesis of poly(pyrrole-co-o-anisidine) on 3102 aluminum alloy and its corrosion protection properties, Mater. Chem. Phys. 125 (2011) 370–376.

[32] R. Solmaz, G. Kardaş, B. Yazıcı, M. Erbil, Adsorption and corrosion inhibitive properties of 2-amino-5-mercapto-1,3,4-thiadiazole on mild steel in hydrochloric acid media, Colloids Surf. A 312 (2008) 7–17.

[33] M.A. Amin, M.A. Ahmed, H.A. Arida, F. Kandemirli, M. Saracoglu, T.Arslan, Monitoring corrosion and corrosion control of iron in HCl by non-ionic surfactants of the TRITON-X series – Part III. Immersion time effects and theoretical studies, Corros. Sci. 53 (2011) 1895–1909.

[34] A. Popova, M. Christov, A. Vasilev, Mono- and dicationic benzothiazolic quaternary ammonium bromides as mild steel corrosion inhibitors. Part II: Electrochemical impedance and polarization resistance results, Corros. Sci. 53 (2011) 1770–1777.

[35] R. Solmaz, M.E. Mert, G. Kardaş, B. Yazıcı, M. Erbil, Adsorption and corrosion inhibition effect of 1,1-thiocarbonyldiimidazole on mild steel in H_2SO_4 solution and synergistic effect of iodide ion, Acta Physico-Chim. Sin. 24 (2008) 1185–1191.

[36] D. Risovic, S.M. Poljac, K. Furic, M. Gojo, Inferring fractal dimension of rough/porous surfaces – a comparison of SEM image analysis and electrochemical impedance spectroscopy methods, Appl. Surf. Sci. 255 (2008) 3063–3070.

[37] T. Pajkossy, Impedance spectroscopy at interfaces of metals and aqueous solutions – surface roughness CPE and related issues, Solid State Ionics 176 (2005) 1997–2003.

[38] S.S. Abdel Rehim, H.H. Hassan, M.A. Amin, Corrosion and corrosion inhibition of Al and some alloys in sulphate solutions containing halide ions investigated by an impedance technique, Appl. Surf. Sci. 187 (2002) 279–290.

[39] F. Bentiss, M. Traisnel, N. Chaibi, B. Mernari, H. Vezin, M. Lagrenee, 2,5-Bis(n-methoxyphenyl)-1,3,4-oxadiazoles used as corrosion inhibitors in acidic media: correlation between inhibition efficiency and chemical structure, Corros. Sci. 44 (2002) 2271–2289.

[40] A.K. Singh, M.A. Quraishi, The effect of some bis-thiadiazole derivatives on the corrosion of mild steel in hydrochloric acid, Corros. Sci. 52 (2010) 1373–1385.

[41] A. Döner, R. Solmaz, M. Özcan, G. Kardaş, Experimental and theoretical studies of thiazoles as corrosion inhibitors for mild steel in sulphuric acid solution, Corros. Sci. 53 (2011) 2902–2913.

[42] W. Li, Q. He, S. Zhang, C. Pei, B. Hou, Some new triazole derivatives as inhibitors for mild steel corrosion in acidic medium, J. Appl. Electrochem. 38 (2008) 289–295.

[43] M. Behpour, S.M. Ghoreishi, N. Mohammadi, M. Salavati-Niasari, Investigation of the inhibiting effect of *N*-[(*Z*)-1-phenylemethyleidene]-*N*-{2-[(2-{[(*Z*)-1phenylmethylidene]amino}phenyl)disulfanyl]phenyl} amine and its derivatives on the corrosion of stainless steel 304 in acid media, Corros. Sci. 53 (2011) 3380–3387.

[44] V.V. Torres, R.S. Amado, C. Faia de Sa, T.L. Fernandez, C.A.S. Riehl, A.G. Torres, E. D'Elia, Inhibitory action of aqueous coffee ground extracts on the corrosion of carbon steel in HCl solution, Corros. Sci. 53 (2011) 2385–2392.

[45] M.A. Hegazy, H.M. Ahmed, A.S. El-Tabei, Investigation of the inhibitive effect of p-substituted 4-(*N*,*N*,*N*-dimethyldodecylammonium bromide)benzylidene-benzene-2-yl-amine on corrosion of carbon steel pipelines in acidic medium, Corros. Sci. 53 (2011) 671–678.

[46] E.L. Bettini, Progress in Corrosion Research, Nova Science Publishers, New York, 2007. 193pp..

[47] E.V. Pereira, R.B. Figueira, Manuela M. Salta, I.T.E. Fonseca, Long-term efficiency of two organic corrosion inhibitors for reinforced concrete, J. Mater. Sci. Forum 636–637 (2010) 1059–1064.

[48] D. Mohammedi, A. Benmoussa, C. Fiaud, E.M.M. Sutter, Synergistic or additive corrosion inhibition of mild steel by a mixture of HEDP and metasilicate at pH 7 and 11, Mater. Corros. 11 (2004) 55.

[49] F. Bentiss, M. Lebrini, M. Lagrenee, M. Traisnel, A. Elfarouk, H. Vezin, The influence of some new 2,5-disubstituted 1,3,4-thiadiazoles on the corrosion behaviour of mild steel in 1 M HCl solution: AC impedance study and theoretical approach, Electrochim. Acta 52 (2007) 6865–6872.

[50] J. Aljourani, K. Raeissi, M.A. Golozar, Benzimidazole and its derivatives as corrosion inhibitors for mild steel in 1 M HCl solution, Corros. Sci. 51 (2009) 1836–1843.

[51] Z. Tao, S. Zhang, W. Li, B. Hou, Corrosion inhibition of mild steel in acidic solution by some oxo-triazole derivatives, Corros. Sci. 51 (2009) 2588–2595.

[52] S.A. Abd El-Maksoud, A.S. Fouda, Some pyridine derivatives as corrosion inhibitors for carbon steel in acidic medium, Mater. Chem. Phys. 93 (2005) 84–90.

[53] X. Li, S. Deng, H. Fu, Triazolyl blue tetrazolium bromide as a novel corrosion inhibitor for steel in HCl and H_2SO_4 solutions, Corros. Sci. 53 (2011) 302–309.

[54] A.K. Satapathy, G. Gunasekaran, S.C. Sahoo Kumar Amit, P.V. Rodrigues, Corrosion inhibition by *Justicia gendarussa* plant extract in hydrochloric acid solution, Corros. Sci. 51 (2009) 2848–2856.

[55] F. Bentiss, M. Lebrini, M. Lagrenee, Thermodynamic characterization of metal dissolution and inhibitor adsorption processes in mild steel/2,5-bis(n-thienyl)-1,3,4-thiadiazoles/hydrochloric acid system, Corros. Sci. 47 (2005) 2915–2931.

[56] G. Moretti, F. Guidi, G. Grion, Tryptamine as a green iron corrosion inhibitor in 0.5 M deaerated sulphuric acid, Corros. Sci. 46 (2004) 387–403.

[57] H. Ashassi-Sorkhabi, B. Shaabani, D. Seifzadeh, Corrosion inhibition of mild steel by some schiff base compounds in hydrochloric acid, Appl. Surf. Sci. 239 (2005) 154–164.

[58] Y.P. Khodyrev, E.S. Batyeva, E.K. Badeeva, E.V. Platova, L. Tiwari, O.G. Sinyashin, The inhibition action of ammonium salts of *O*,*O*-dialkyldithiophosphoric acid on carbon dioxide corrosion of mild steel, Corros. Sci. 53 (2011) 976–983.